

PHENOMENOLOGICAL AND PREDICTIVE STUDIES OF CONFINEMENT
AND GLOBAL HEATING IN JET NEUTRAL BEAM HEATED LIMITER PLASMAS

E Thompson, D Bartlett, F Bombarda(1), G Bracco(1), D J Campbell, C Challis, J P Christiansen, J G Cordey, S Corti, A Costley, G Duesing, R Giannella(1), A P H Goede, L Horton, T T C Jones, E Kallne, O Kaneko(2), P J Lomas, D Muir, J Snipes, A Staebler(3), D Stork, P M Stubberfield, G Tallents, P R Thomas, K Thomsen, M von Hellerman and M L Watkins.

JET Joint Undertaking, Abingdon, U.K., (1) EURATOM-ENEA Association, Frascati, Italy, (2) Institute of Plasma Physics, Nagoya, Japan, (3) IPP Garching, FRG.

INTRODUCTION

NBI experiments have been performed using a wide range of target plasmas to establish the scaling of the global energy confinement with plasma current (I_p), toroidal magnetic field (B_T) plasma density (n_e) and input power (P_{TOT}) for both H^0 (≤ 65 keV) & D^0 (≤ 80 keV) injection into D plasmas. This paper describes results obtained with the plasma boundary defined by either the 8 outboard graphite limiters, or by the graphite inner wall protection tiles. The results of NBI experiments in X-point plasmas are presented elsewhere [1].

The JET vacuum vessel and graphite surfaces are conditioned by baking and glow discharge cleaning. They were maintained at 290°C during these experiments. The plasma density behaviour during NBI varied according to limiter configuration and is described in [2]. In summary the onset of NBI led to a transient density increase under all conditions. For outboard limiters the density rises linearly during NBI. On the inner wall tiles, a much lower density increase was obtained. This pumping was further improved during the 'hot-ion' campaign by conditioning the inner wall surfaces using Helium Ohmic discharges prior to NBI discharges.

GLOBAL ENERGY CONFINEMENT

The total plasma energy content from diamagnetic loop measurements (W^{DIA}) of all NBI plasmas is well described by a linear function of P_{TOT} when all other controllable parameters are constant [3]. Energy contents determined from poloidal field measurements and kinetic pressure profiles show similar behaviour and the three stored energy measurements are in reasonable agreement. The energy contents are roughly proportional to plasma current. These dependences have been built into an offset linear scaling law [3] of the form (figure 1)

$$W^{DIA} = 0.225 n_e^{0.6} I_p^{0.5} B_T^{0.4} + 0.047 I_p P_{TOT} \quad (1).$$

The scaling of the energy content of Ohmic discharges is reproduced by the scaling of the intercept in (1). The dependence of W on the relevant parameters is described equally well by a power law fit, which is shown in figure 2

$$W^{DIA} = 0.27 P_{TOT}^{0.37} I_p^{0.67} \langle n_e \rangle^{0.41} B_T^{0.24} \quad (2)$$

The data is also well described by L-mode scaling [5].

From local transport analysis [4] which includes the NBI power deposition profile it can be concluded that the plasma thermal conductivity apparently depends upon the poloidal field only. The 3 MA data obtained after He conditioning were not used in the above fitting procedure and they exhibit higher values of τ_{inc} ($= \delta W / \delta P_{TOT}$) than high density pulses. The measured density profiles of these discharges also show a tendency towards being slightly more peaked than other types of NI discharges.

Heating Efficiency with NBI

NBI electron heating efficiency on JET has been constrained by the relatively low values of injection energy (30-60 keV/AMU). The electron heating efficiency (figure 3) tends to saturate at electron temperature values 5-6 keV where the total power input to the electrons (NBI + Ohmic + Equipartition) has fallen to a low level.

In contrast, ion heating efficiency increases with the power per particle (figure 4). The spectroscopic N_1^{26+} temperature measurements shown in figure 4 are calculated to be at most 1-2 keV higher than the deuterium temperature at the highest values. The discharges following helium conditioning show the best ion heating, partly because lower densities are accessible than in limiter discharges. This results in the decoupling of the ions from the electrons as the equipartition time (τ_{ei}) becomes larger than the energy confinement time.

These 'High T_i ' discharges gave the highest neutron rate obtained on JET ($2.8 \cdot 10^{15} \text{ s}^{-1}$) of which approximately half can be attributed to beam-plasma reactions.

Enhanced Confinement in Inner Wall Discharges

The energy content of the inner wall (3 MA, 3.4 T) plasmas falls into 2 groups ('A' and 'B' in figure 5). The type A plasmas were those immediately following helium conditioning. They showed reduced recycling evidenced by a steady-state density and the lowest values of deuterium- α light during NBI.

The measured electron energy contents (W_e) in the two groups were identical within errors so the difference in W_{DIA} must reside in the ions. The calculation of stored energy using the measured central ion temperature and dilution factor from the measured Z_{eff} indicates that the ion temperature profile was more peaked than that of the electrons in these shots. This is confirmed by preliminary results obtained by a neutral particle analyser array.

Power Balance in Hot Ion Plasmas

The data for 3.0 MA/3.4 T plasmas with $5.0 < P_{TOT} < 7.0$ MW has been compared with results from a simple 0-D model. The model uses characteristic times based on L-mode scaling for loss rates in both channels and classical equipartition between them. The predictions of this model reproduce the data tolerably well (figure 6). This indicates the energy confinement is no different in character between hot ion and high density regimes.

Local transport analysis is limited by the preliminary nature of ion temperature profiles, nevertheless the available data does show that, in

contrast to high density plasmas, the ion loss channel dominates within the central half minor radius in hot ion plasmas. Ion convection and conduction have comparable magnitudes in the centre and equipartition returns a large power fraction to the electrons in the outer plasma. In these respects JET hot ion plasmas are similar to TFTR supershots [6].

REFERENCES

- [1] Keilhacker M, et al, these proceedings.
- [2] Jones TTC, et al, these proceedings.
- [3] Cordey JG, et al, 11th Int. Conf. on Plasma Phys. & Contr. Nucl. Fus. Research (Kyoto 1986), IAEA-CN-47/QA-II-3.
- [4] Callen J, et al, 'Modelling of temperature profile responses to Heating Profiles in JET', these proceedings.
- [5] Goldston RJ, Plasma Phys. & Contr. Fus. 26,1A,87-103 (1984).
- [6] Hawryluk RJ, et al, 11th Int. Conf. on Plasma Phys. & Contr. Nucl. Fus. Research (Kyoto 1986), IAEA-CN-47/A-I-3.

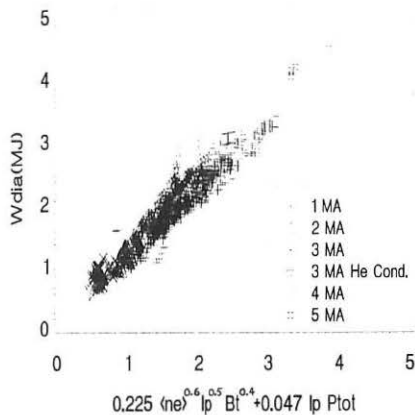


Figure 1 : Offset linear scaling law plotted against JET NBI stored energy measured by diamagnetic loop (W^{DIA}).

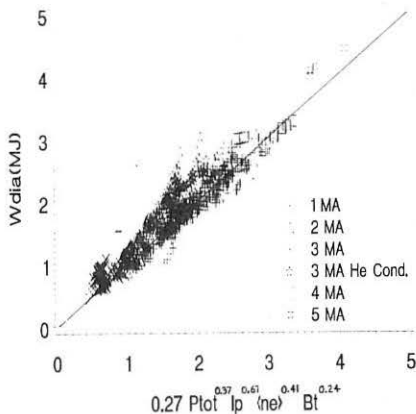


Figure 2 : Power law fit to NBI W^{DIA} measurements.

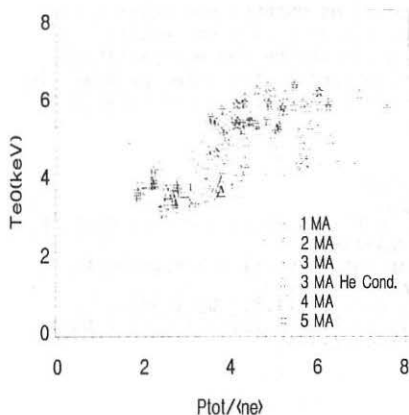


Figure 3 : Central electron temperature from ECE measurements for NBI discharges as a function of total power (P_{tot}) normalised by volume averaged density ($\langle n_e \rangle$).

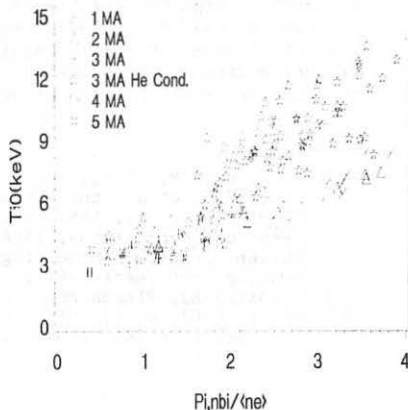


Figure 4 : Central ion temperature ($T_i(o)$) for Ni^{26+} ions in NBI discharges measured by Doppler shift of the NiXXVII line as a function of calculated power to the ions (P_{bi}) normalised by volume averaged density ($\langle n_e \rangle$).

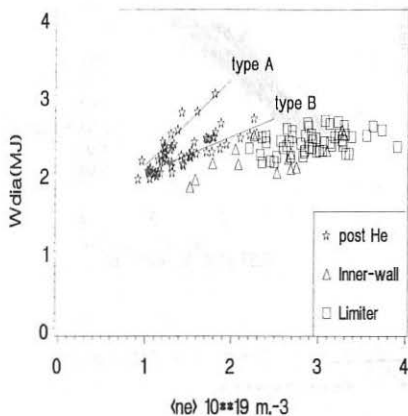


Figure 5 : Diamagnetic stored energy measured as a function of volume averaged density for 3 MA/3.4 T NBI discharges.

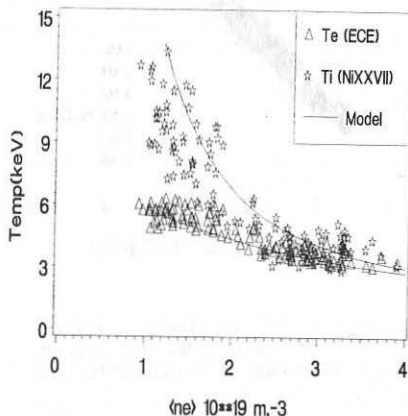


Figure 6 : Measured $T_i(o)$ and $T_e(o)$ for NBI discharges compared to predictions from the simple O-D code (see text).